Spectroscopy of ^{35}P using the one-proton knockout reaction

A. Mutschler, O. Sorlin, A. Lemasson, Dominique Bazin, C. Borcea, R. Borcea, A. Gade, H. Iwasaki, E. Khan, A. Lepailleur, et al.

Spectroscopy of ^{35}P using the one-proton knockout reaction

A. Mutschler,[1,2] O. Sorlin,[2] A. Lemasson,[2,3] D. Bazin,[3] C. Borcea,[4] R. Borcea,[4] A. Gade,[3] H. Iwasaki,[3] E. Khan,[1] A. Lepailleur,[2] F. Recchia,[3] T. Roger,[2] F. Rotaru,[4] M. Stanoiu,[4] S. R. Stroberg,[3,5] J. A. Tostevin,[6] M. Vandebrouck,[1,2] D. Weisshaar,[3] and K. Wimmer[7,8,3]

[1]*Institut de Physique Nucléaire, IN2P3-CNRS, F-91406 Orsay Cedex, France*
[2]*Grand Accélérateur National d'Ions Lourds (GANIL), CEA/DSM - CNRS/IN2P3, B. P. 55027, F-14076 Caen Cedex 5, France*
[3]*Department of Physics and Astronomy and National Superconducting Cyclotron Laboratory, Michigan State University, East Lansing, Michigan, 48824-1321, USA*
[4]*IFIN-HH, P. O. Box MG-6, 76900 Bucharest-Magurele, Romania*
[5]*TRIUMF, 4004 Westbrook Mall, Vancouver, British Columbia, V67 2A3 Canada*
[6]*Department of Physics, University of Surrey, Guildford, Surrey GU2 7XH, United Kingdom*
[7]*Department of Physics, The University of Tokyo, Hongo, Bunkyo-ku, Tokyo 113-0033, Japan*
[8]*Department of Physics, Central Michigan University, Mt. Pleasant, Michigan 48859, USA*

(Dated: February 10, 2016)

The structure of ^{35}P was studied with a one-proton knockout reaction at 88 MeV/u from a ^{36}S projectile beam at NSCL. The γ rays from the depopulation of excited states in ^{35}P were detected with GRETINA, while the ^{35}P nuclei were identified event-by-event in the focal plane of the S800 spectrograph. The level scheme of ^{35}P was deduced up to 7.5 MeV using $\gamma - \gamma$ coincidences. The observed levels were attributed to proton removals from the *sd*-shell and also from the deeply-bound $p_{1/2}$ orbital. The orbital angular momentum of each state was derived from the comparison between experimental and calculated shapes of individual (γ-gated) parallel momentum distributions. Despite the use of different reactions and their associate models, spectroscopic factors, C^2S, derived from the ^{36}S $(-1p)$ knockout reaction agree with those obtained earlier from ^{36}S(d,^{3}He) transfer, if a reduction factor R_s, as deduced from inclusive one-nucleon removal cross sections, is applied to the knockout transitions. In addition to the expected proton-hole configurations, other states were observed with individual cross sections of the order of 0.5 mb. Based on their shifted parallel momentum distributions, their decay modes to negative parity states, their high excitation energy (around 4.7 MeV) and the fact that they were not observed in the (d,^{3}He) reaction, we propose that they may result from a two-step mechanism or a nucleon-exchange reaction with subsequent neutron evaporation. Regardless of the mechanism, that could not yet be clarified, these states likely correspond to neutron core excitations in ^{35}P. This newly-identified pathway, although weak, offers the possibility to selectively populate certain intruder configurations that are otherwise hard to produce and identify.

PACS numbers: 24.50.+g,25.60.Gc,21.10.Jx,25.60.Lg

I. INTRODUCTION.

For many decades, single nucleon transfer reactions have been one of the tools of choice for the study of shell structure in nuclei. Various combinations of light projectiles were used on stable targets to probe occupied single-particle levels and valence states, e.g. the (d, p) neutron-adding transfer to study the valence neutron shell and the (d,^{3}He) proton-removing transfer to study occupied proton orbitals. At facilities where radioactive ion beams are available with sufficient intensity, this approach is also now used for unstable nuclei in inverse kinematics, probing those active orbitals near the Fermi surface. Separation energies and orbital angular momenta and the occupation of nucleon orbitals in the nucleus of interest are extracted from the energy and angular distributions of the light ejectile and from the sum of partial cross sections, respectively. Using direct reaction theory, this is done in a model-dependent way, including the use of appropriate optical potentials in the entrance and exit channels. The magnitudes and evolution of shell gaps and the softness or stiffness of the nuclear Fermi surfaces were studied on many stable (and recently also on a few unstable) nuclei using these techniques (see e.g. Refs [1, 2] for results on the stable ^{40}Ca and ^{48}Ca nuclei).

Even for closed-shell nuclei, short-range correlations [3] and coupling to collective degrees of freedom [4] complicate the determination of single-particle energies and spectroscopic factors (or their related shell occupancies and vacancies) which are not directly observable [5, 6]. Furthermore, reaction models exploit *effective* potentials that do not capture the full microscopic complexity of the nucleus and shell-model interpretations can depend strongly on truncations of the valence space. As a result, values of spectroscopic factors, C^2S, deduced experimentally are quenched compared to theoretical calculations. This quenching is typically a factor of about $R_s = 0.55(10)$ [7, 8] in stable and near-stable nuclei.

Strictly speaking, the only *true* experimental observables are the energies of levels in the final nucleus and their partial feeding cross sections. However, to interpret

the underlying nuclear structure it is important to infer shell evolution and occupancies from these observables. Assuming collective coupling (e.g. to giant resonances) and short-range correlation effects are similar between neighboring nuclei, consideration of the *differential* evolution of single-particle energies, spectroscopic strengths and occupancies is sensible, a view supported by their successful use up to now.

With the development of accelerator facilities producing intense high-energy secondary beams of rare isotopes at energies of around 100 MeV/u or more, the linear and angular momentum matching of light-ion-induced pick-up or stripping reactions is poor, resulting in small cross sections of the order of 1 mb. With thin targets, this technique is then only applicable for the most intense beams. A higher-luminosity alternative, the intermediate-energy nucleon knockout reaction, is also being exploited successfully to study the spectroscopy of extremely neutron-rich or deficient nuclei. Being sensitive to the same single-nucleon overlaps, empirical proton and neutron spectroscopic factors $C^2S(\alpha)$ to bound states α in the residual, mass $(A-1)$, nucleus can be deduced from partial cross-section measurements [9, 10]. For near-stable nuclei with modest proton to neutron separation energy asymmetry, i.e. $|\Delta S| = |S_p - S_n| < 10$ MeV, fast proton knockout, $(d,^3\mathrm{He})$ and electron-induced proton knockout (e,e',p) reactions have all been used to populate proton-hole-like final states by proton removal. In each case, reaction model calculations that use shell-model C^2S must be suppressed by very similar factors, R_s, to agree with data [8, 11, 12]; this despite the very different reaction energies, mechanisms, models and approximations involved. In the nuclear knockout case, this suppression has been quantified for many systems at the level of the inclusive cross sections, the summed partial cross sections to all bound final states of the reaction residues. Based on a compilation of this large body of experimental one-proton and one-neutron knockout reactions data on both neutron-rich and neutron-deficient nuclei, a significant variation of the $R_s = \sigma_{exp}/\sigma_{th}$ value (from 0.3 to 1) was observed when systems with extreme ΔS values were explored [12]. So far, this strong trend has not been reported when using (p,d) or $(d,^3\mathrm{He})$ reactions in the few systems studied with significant ΔS asymmetry [13, 14], potentially the result of large uncertainties in the transfer reaction theory [15] for such highly-mismatched transitions.

An aim of the present work is to compare the states populated, their deduced angular momenta and their C^2S values as extracted from the one-proton knockout reaction $^{36}\mathrm{S}(-1p)^{35}\mathrm{P}$ with those from the $^{36}\mathrm{S}(d,^3\mathrm{He})^{35}\mathrm{P}$ stripping reaction [16]. This study covers proton separation energies that differ by 10 MeV, from the removal of the most deeply-bound proton from the $1p_{1/2}$ orbital to removal of a $1d_{3/2}$ valence proton from ^{36}S. This work shows that the one-proton knockout and $(d,^3\mathrm{He})$ transfer reactions can be analyzed to extract consistent spectroscopic information. Furthermore, a few percent of the observed cross section leads to suspected negative parity states that cannot be interpreted as due to the direct one-proton knockout reaction. Their origin will be discussed in the final part of the manuscript.

II. EXPERIMENTAL PROCEDURE

A secondary beam of ^{36}S was produced in the fragmentation of a 140 MeV/u ^{48}Ca primary beam on a 846 mg/cm^2 ^{9}Be target, delivered by the coupled cyclotron facility at NSCL. The ^{36}S nuclei were selected with the A1900 fragment separator [17, 18], yielding an average intensity and purity of 8.1 10^5 s^{-1} and 89.7%, respectively. The constituents in the projectile beam were identified from their time-of-flight difference provided by two plastic scintillators located before the secondary target. The 100-mg/cm^2 secondary target of ^{9}Be was located at the reaction target position of the S800 spectrograph whose magnetic rigidity was centered on the ^{35}P residues produced in the one-proton knockout from the ^{36}S projectiles. The projectile-like reaction residues were identified on an event-by-event basis from their energy loss measured in an ionization chamber located at the focal plane of the S800 and from their time-of-flight measured between two scintillators situated at the object position and at the focal plane of the S800 spectrometer. The trajectories of the residues were determined from positions and angles determined in the focal plane using two cathode-readout drift chambers [19]. Their non-dispersive position and the momentum vector at the target position were reconstructed using the ray-tracing ion-optics code COSY [20]. A total of $3.7 \cdot 10^6$ ^{35}P nuclei produced from ^{36}S were registered during the measurement.

Prompt γ rays corresponding to the deexcitation of the ^{35}P residues in flight were detected with the seven modules of the Gamma-Ray Energy Tracking In-beam Nuclear Array (GRETINA) [21] that surrounded the secondary target position. Four of the detectors covered the most forward angles centered on 58°, while the remaining three were installed at 90°. Event-by-event Doppler correction was performed using the event-by-event ion velocity and position at mid-target, as well as the γ-ray detection angle derived from the γ-ray interaction position in the segments of the GRETINA array. For this it was assumed that the first interaction point corresponds to the interaction point with highest energy deposition (main interaction scheme). The energies of γ rays detected in the same or neighboring crystals were considered to come from one single event. They were summed in an add-back procedure to increase the γ-ray efficiency in particular at high energy. These add-back spectra were used also to establish the level scheme of ^{35}P using γ-γ coincidence from the full GRETINA array using all angles. Absolute γ-ray intensities and deduced final-state populations were derived without add-back from the modules at 90° only, since – at the very high projectile rates of close to 1 MHz – the forward detectors were exposed to frequent

high-energy events likely induced by light particles [22], causing preamplifier saturation and preventing a reliable deadtime determination for these detectors.

Gamma-ray efficiencies were determined up to 1.4 MeV using a calibrated ^{152}Eu γ-ray source. Absolute γ-ray efficiencies extrapolated to higher energies and that take the Lorentz boost from the in-flight emission of the γ-ray into account were obtained from GEANT4 simulations [23], yielding simulated efficiencies of 5.5% (7%) at 1 MeV without (with) add-back. Gamma-ray energy centroids were determined with an uncertainty of 2 keV.

III. LEVEL SCHEME OF ^{35}P

The Doppler-corrected singles γ-ray spectrum of ^{35}P is shown in the first row of Fig. 1 for two energy ranges spanning up to 10 MeV. Owing to the high γ-ray detection efficiency, photo peaks are still observed up to 7.5 MeV, well above the known γ rays observed so far in this nucleus, and close to the neutron separation energy of S_n = 8.38 MeV. The γ-ray spectra of ^{35}P, gated on the 391, 1473, 2386, 3860 and 1995 keV lines, are shown in the second to fourth rows of Fig. 1. The γ-γ coincidences deduced from these spectra have been used to establish the level scheme of ^{35}P. The deduced fractional population of each level, b_f, is given in Fig. 2 in units of %.

Interestingly, all the levels displayed with black lines in Fig. 2 that have a significant feeding were also populated in the ^{36}S(d,^{3}He)^{35}P reaction performed in normal kinematics and at low energy [16]. There, the positive-parity states, the $1/2^+$ (g.s.) and the $5/2^+$ states (3860, 4665, 5197 keV) were interpreted as hole configurations originating from the removal of a proton from the occupied $2s_{1/2}$ and $1d_{5/2}$ orbitals in ^{36}S, respectively, while the observed $3/2^+$ (2386 keV) was proposed to correspond to a proton excitation into the $1d_{3/2}$ orbital. No spin assignment was proposed for the highest energy levels at 5709 keV (not observed in Ref. [16]) and at 7526 keV, which we propose to correspond to hole configurations involving the deeply-bound $p_{1/2}$ orbital, as discussed later. Regardless of the spin assignments and spectroscopic factor values that will be discussed in the next section, this shows that the (d,^{3}He) transfer reaction and the one-proton knockout reaction populate the same states in ^{35}P. Since derived from high-resolution spectroscopy of γ rays, the energies of these states are more accurate than the ones from the transfer reaction for which uncertainties of about 20 keV were reported.

The states at 4101 and 4494 keV were reported in Ref. [24] from the β-decay of ^{35}Si to ^{35}P as well as in Ref. [25] using the ^{208}Pb(^{36}S,X+γ) reaction at 230 MeV. States at 5560 and 6096 keV that were proposed to be populated in the β decay are neither observed in the present experiment, nor in Ref. [25]. As for the 5560 keV state, it is most likely not populated in our experiment since we do not observe any evidence for the 3174-keV

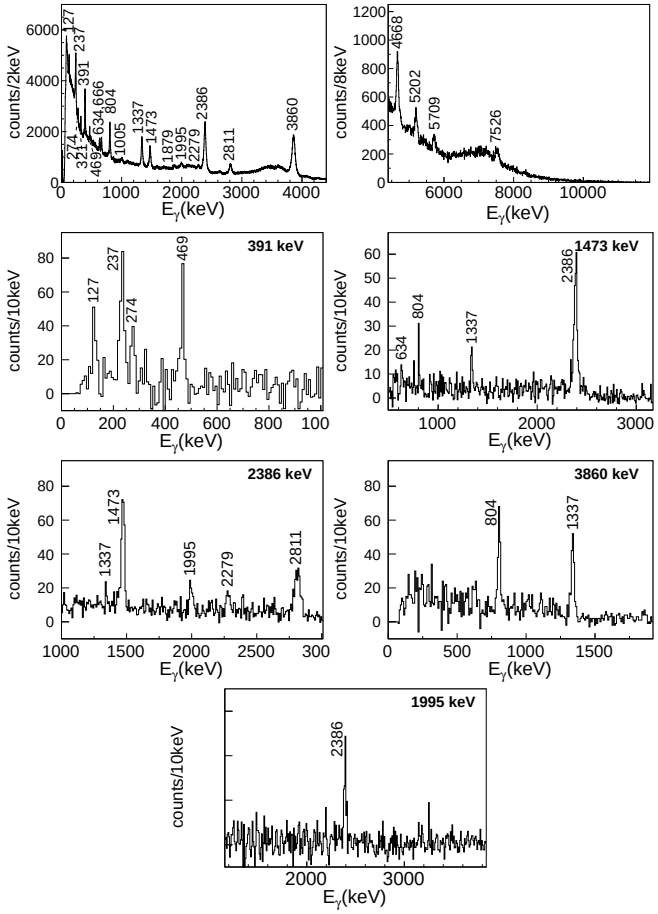

FIG. 1: Singles (first line) and γ-gated (second to fourth lines) γ-ray Doppler-corrected spectra of ^{35}P.

γ-ray branch deexciting it. The 6096-keV state was proposed to decay with a 1995 keV transition, followed by cascades containing 241, 1473, 1715, 2386, 3860 and 4101 keV γ rays. In our work, as in Ref. [25], the 1995-keV transition is in coincidence with the 2386-keV line but not with any other of the observed transitions at 237, 1473 and 3860 keV. We therefore suggest that our reported 4382-keV state (4381 keV in [25]) is the origin of the 1995-keV γ ray transition and that the suggested 6096-keV level reported from the β-decay experiment [24] was likely wrongly placed. In order to match allowed β-decay Gamow-Teller selection rules, the states at 4101, 4382 and 4494 keV, fed from the J$^\pi$=7/2$^-$ g.s. of ^{35}Si, should have $5/2^- \leqslant$ J $^\pi \leqslant 9/2^-$ spin and parity assignments.

The states at 4382, 4766, 4960 and 5087 keV, indicated in red in Fig. 2, were already identified in Ref. [25]. They are populated in our experiment with rather weak individual fractions, b_f, of around 1-2%, at a total of 4.7%, but were not observed with the (d,^{3}He) transfer reaction [16]. This could either be due to the better sensitivity of the present experiment as compared to the work of [16], or it could point to the fact that these states are not pop-

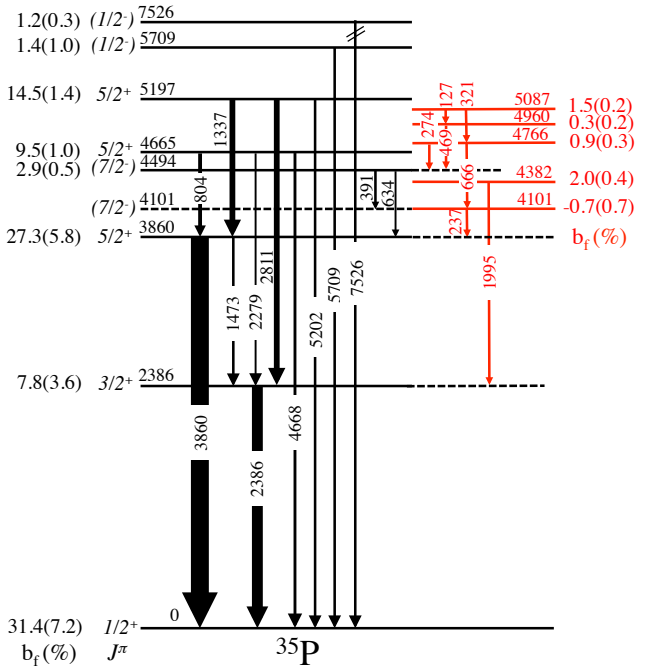

FIG. 2: (color on line) (a) Energies (with uncertainties of σ=2 keV) and population fractions, b_f (in %) of the states fed in ^{35}P during our experiment, by the one proton-knockout reaction (in black), or possibly by a two-step reaction mechanism (right part, in red), see text for details. The reported spins and parities of states, taken from Ref. [25], are confirmed by the present work.

ulated in the one-proton knockout reaction but rather by another process. To shed light on this unexpected feature, we first note that these states mostly decay by low-energy γ rays to each other or to previously-suggested negative-parity $7/2^-$ states at 4101 and 4494 keV rather than by high-energy transitions to lower-lying positive-parity low-spin states. One may therefore suspect that they have negative parity or/and spin values larger or equal to $J = 5/2$. As these states are located at energies similar to the J^π=3$^-$,4$^-$,5$^-$ states in ^{36}S that correspond to neutron core excitations $(d_{3/2})^{-1}(f_{7/2})^{+1}$, one may suspect that they have the same origin. These neutron core excitations could not be populated through a direct one-proton knockout reaction but must rather come from another process, as will be discussed in Section V B.

IV. KNOCKOUT REACTION CALCULATIONS

The eikonal model and the choice of parameters used to calculate the proton-removal single-particle cross sections, σ_α^{sp}, to residue final states α – the cross sections for removal of a proton with quantum numbers α=n, ℓ, J and unit spectroscopic factor – are detailed in Ref. [26]. These σ_α^{sp}, each the sum of stripping and diffractive removal contributions, are computed based on the radial overlaps of the initial and final state wave functions and the ^{35}P residue- and proton-target elastic S-matrices calculated from their complex optical interactions with the ^{9}Be target [27]. These S-matrices are calculated in the double- and single-folding model (optical) limit of Glauber's multiple-scattering theory. The residue-target interaction uses the proton and neutron densities of ^{35}P from Skyrme (SkX interaction [28]) Hartree-Fock (HF) calculations. The ^{9}Be target density is a Gaussian with a root-mean-squared (rms) radius of 2.36 fm. The removed proton-^{35}P relative motion wave functions (radial overlaps) and their single-particle rms radii are also constrained, consistently, by HF calculations (see [26] for further details).

Systematic analyses have been made of an increasing body of precision inclusive nucleon knockout (KO) data by consistent use of this methodology combined with the shell-model spectroscopy (levels and spectroscopic factors) appropriate to each case. These systematics, summarized recently in Ref. [12], show a clear correlation of the ratio of the experimental to the theoretical (eikonal plus shell-model) inclusive knockout cross sections, $R_s = \sigma^{exp}_{inc,KO}/\sigma^{th}_{inc,KO}$, with the asymmetry $\Delta S = S_p - S_n$ of the proton (S_p) and neutron (S_n) separation energies from the projectile. For proton knockout reactions this dependence can be parameterised as

$$R_s = -0.016[S_p - S_n] + 0.61 \qquad (1)$$

with an associated error of order 20%.

As discussed in the previous section, the measured partial cross section to each final state f of ^{35}P is $\sigma_f = b_f\,\sigma^{exp}_{inc}$, where 95.3% of the total inclusive cross section, σ^{exp}_{inc}, is attributed to states populated by the direct proton knockout mechanism. Thus, for the dominant KO final states, $\sigma_f = b_f\,\sigma^{exp}_{inc} = b_f^{KO}\,\sigma^{exp}_{inc,KO}$, where $b_f^{KO} = b_f/0.953$ and $\sigma^{exp}_{inc,KO}$ is the measured inclusive KO cross section, as enters the definition of R_s.

In the present work we deduce (normalized) proton spectroscopic factors for the individual KO final states f (with excitation energy E^*) from the measured partial cross sections and the calculated single particle cross sections, as follows:

$$C^2S^{exp}_{norm} = \frac{b_f^{KO}\sigma^{exp}_{inc,KO}}{R_s\sigma^{sp}_f}. \qquad (2)$$

In calculating these $C^2S^{exp}_{norm}$, the R_s trend from the inclusive data, Eq. (1), is now used for each final state and is calculated for the proton separation energy to that state, i.e. $S_p = S_p(g.s.) + E^*$. As we observe excited states with E^* up to 7.5 MeV, R_s varies by about 20% over this range. We note that if a constant (inclusive) R_s value had been used for all final states, the deduced normalized C^2S values shown in Table I would still agree with those presented within the stated errors. Our use of R_s in the denominator in Eq. (2), means that we extract shell-model-like (and not suppressed) spectroscopic factors that, in a sum-rule limit, can be compared to the occupancies of the active orbits in a finite-basis shell-model

calculation. Thus, as defined, the summed $C^2S^{exp}_{norm}$ for a given J should have a maximum value of $(2J+1)$ in the limit that an orbital with angular momentum J is fully occupied.

The ℓ value of the removed proton is determined by comparing measured parallel momentum distributions ($p_{//}$) of the ^{35}P residues to theoretical distributions calculated with the same S-matrices and overlaps as used for the computation of the σ^{sp}_f [29, 30]. In order to account for broadening effects on $p_{//}$, due to the incoming beam momentum profile and the straggling of the secondary beams that pass through the target, theoretical $p_{//}$ distributions were folded with the experimental $p_{//}$ distribution obtained from the unreacted ^{36}S nuclei passing through the target. Also, the additional momentum broadening induced by the fact that the proton knockout reaction may happen anywhere in the target has been taken into account.

V. RESULTS AND DISCUSSIONS

A. Proton occupancies in ^{36}S

As discussed earlier, the same states were populated in the knockout from ^{36}S to ^{35}P and in the ^{36}S(d,^{3}He) ^{35}P transfer [16] reactions. We now explore whether the deduced spectroscopic factors, C^2S, are also comparable.

The C^2S values obtained from the (d,^{3}He) proton transfer for the $2s_{1/2}$, $1d_{3/2}$, and $1d_{5/2}$ orbits, populating the $1/2^+$, $3/2^+$, $5/2^+$ states in ^{35}P [16] are shown in the final column of Table I. The occupancy of the $2s_{1/2}$ orbit was about 5 times larger than that of the (in a naive picture, unoccupied) $1d_{3/2}$ orbit. Their summed occupancy amounts to about 2. In an extreme single-particle picture, this indicates that there are few excitation from the $2s_{1/2}$ to the $1d_{3/2}$ orbit. Five $5/2^+$ states were proposed at higher excitation energy, among which the assignments of the two states at 4474 and 7520 keV were only tentative. By adding all the $(5/2^+)$ strength, an occupancy of 5.95 was found, very close to the sum rule of $2J+1$=6. Altogether, the summed occupancy of the $(2s, 1d)$ orbits derived from the transfer reaction, $\Sigma C^2S \simeq 7.9 \pm 1.6$ [16], exhausts the sum rule of $\Sigma C^2S = 8$. As, with the DWBA model parameters used by the authors, the derived $C^2S^{(d,^3He)}$ exhaust the truncated-basis shell-model sum rule, these (unsuppressed) values should be compared directly with the shell-model and with the normalized values $C^2S^{exp}_{norm}$ from the KO analysis. One should, however, take the $1d_{5/2}$ strength as maximum as the authors of Ref. [16] tentatively proposed to add two levels with ℓ=2 to their sum (the one at 4474(21) keV with C^2S =0.2, the other at 7520(30) keV with C^2S =0.4) for which the angular distributions of the ^{3}He could not be measured. Moreover, a $7/2^-$ negative-parity assignment was later proposed in Ref. [25] for the 4494 keV state. In the following we attempt to clarify this situation with the help of the present data set.

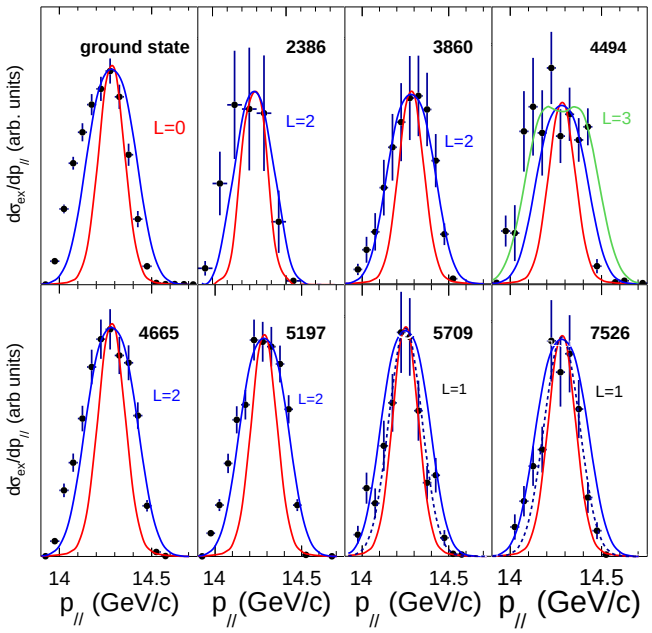

FIG. 3: (color on line) Experimental parallel momentum distributions for the most populated states in ^{35}P (black crosses) are compared to calculations assuming a $\ell = 0$ (red curves), $\ell = 1$ (dashed blue), $\ell = 2$ (blue) and $\ell = 3$ (green) proton removal from the ^{36}S ground state.

Comparisons between experimental and theoretical $p_{//}$ distributions are shown in the panels of Fig. 3 for the states represented in the left hand side of Fig. 2 (with black lines) and populated with b_f values having a statistical significance of at least a 3 σ. Comparison should focus on the high-momentum part of the distributions as the low momentum part exhibits a tail, attributed to events in which energy is dissipated in exciting the target [22], the kinematics of which are not correctly treated by the eikonal model. The three $5/2^+$ excited states at 3860, 4665 and 5197 keV exhibit experimental $p_{//}$ distributions that are compatible with calculated distributions computed for ℓ=2 proton removal. Though the statistics are limited, the $p_{//}$ distribution corresponding to the 4494 keV seems more consistent with an ℓ=3 assignment. It likely corresponds to the state observed, but unassigned, at 4474(21) keV in Ref. [16]. The newly identified state at 5709 keV and the previously unassigned state at 7520(30) keV in [16] display $p_{//}$ distributions in closer agreement with ℓ=1, most likely corresponding to deep-hole configurations involving the $1p_{1/2}$ orbital. No direct feeding of the state at 4101 keV is observed, in agreement with its non-feeding in the (d,^{3}He) reaction [16]. Finally, the $p_{//}$ distribution leading to the ground state is in agreement with an ℓ=0 proton removal and its corresponding $J^\pi = 1/2^+$ assignment. As the population fraction b_f for the ground state is obtained by subtracting the contributions of all excited states, its uncertainty

TABLE I: Energy, spin parity, partial cross-sections ($b_f^{KO} \times \sigma_{inc,KO}^{exp}$), and normalized experimental spectroscopic factors $C^2S_{norm}^{exp}$ of ^{35}P final states populated in the ^{36}S($-1p$) reaction. The spectroscopic factors derived from the (d,^{3}He) transfer reaction [16] are shown in the last column.

E (keV)	J$^\pi$	b_f^{KO} † (%)	$b_f^{KO} \times \sigma_{inc,KO}^{exp}$ (mb)	σ^{sp} (mb)	R_s	$C^2S_{norm}^{exp}$ ‡	$C^2S^{(d,^3He)}$
0	$\frac{1}{2}^+$	32.9(7.5)	16.0(3.6)	13.5	0.55(11)	2.2(7)	1.6(3)
2386	$\frac{3}{2}^+$	8.2(3.8)	4.0(1.8)	10.2	0.52(10)	0.7(3)	0.31(6)
3860	$\frac{5}{2}^+$	28.6(6.1)	13.9(3.0)	10.6	0.49(10)	2.7(8)	2.9(6)
4494	$(\frac{7}{2}^-)$	3.0(5)	1.5(2)	10.7	0.48(10)	0.30(7)	<0.2 ⋆
4665	$\frac{5}{2}^+$	9.9(1.1)	4.8(5)	10.3	0.47(9)	1.0(2)	1.1(2)
5197	$\frac{5}{2}^+$	15.2(1.5)	7.4(7)	10.2	0.47(9)	1.5(3)	1.4(3)
5709	$(\frac{1}{2}^-)$	1.5(1.1)	0.73(53)	10.8	0.47(9)	0.21(16)	-
7526	$(\frac{1}{2}^-)$	1.3(3)	0.63(15)	10.2	0.44(9)	0.20(6)	<0.4 ⋆

† Normalized to have the sum of ($-1p$) knockout events =100%
‡ Normalized according to Eq. (2), and hence the $C^2S_{norm}^{exp}$ sum to $(2J+1)$ in the case of a fully occupied sub-shell.
⋆ Value obtained in [16] by tentatively assuming a $d_{5/2}$ proton transfer.

is large. The ℓ assignments for the most strongly populated states agree with those from the transfer reaction [16]. New tentative assignments are proposed in Table I for the previously unassigned states at 4494 and 7520 keV and the newly identified state at 5709 keV.

The measured inclusive cross section that leads to ^{35}P, from incoming ^{36}S projectiles, is 51(1) mb, of which 95.3 % corresponds to the direct proton knockout (KO) process. The corresponding partial cross sections, $b_f^{KO} \times \sigma_{inc,KO}^{exp}$, as well as the derived $C^2S_{norm}^{exp}$ values, are reported in Table I. All of these $C^2S_{norm}^{exp}$ values are, within the error bars, consistent with those for $C^2S^{(d,^3He)}$ [16]. Thus, despite the use of the different reaction mechanisms and theoretical models, consistent proton spectroscopic factors could be derived using the one-proton knockout and the (d,^{3}He) reaction probes.

B. States in ^{35}P produced by another mechanism

As shown in Fig. 4, the $p_{//}$ centroids for those ^{35}P final states indicated in red on the right hand side of the level scheme in Fig. 2, are systematically shifted to a lower momentum compared to all distributions earlier attributed to the one-proton knockout reaction. It is interesting to compare these centroids with that obtained for ^{36}P produced from ^{36}S in a ^{9}Be-induced nucleon-exchange reaction [31]. In Fig. 4, it is shown that the momentum-shifted centroids of ^{35}P match the one deduced from the experimental $p_{//}$ distribution of ^{36}P after being scaled by a factor of 35/36, that would correspond to the evaporation of one neutron following nucleon exchange into ^{36}P. Having similar cross sections, the states in ^{36}P (σ= 1.5(5) mb) and the momentum-shifted ones in ^{35}P (σ=2.40(4) mb), are likely populated by the same nucleon-exchange mechanism. It is conceivable that these states are reached either by: (i) a two-step (TS) process involving a proton knockout and a neutron pickup, or (ii) a charge-exchange (CE) reaction. Either way, bound or unbound states may be produced in ^{36}P, leading to characteristic γ rays in ^{36}P or decay to ^{35}P, respectively. These states could also be produced, as proposed in Ref. [22], by a (iii) TS reaction pathway in which the ^{36}S core is excited by inelastic scattering with proton removal from the excited state. These three possibilities are examined in the following.

When assuming that the knockout and pickup reactions have a similar dependence on impact parameter, the cross section for a TS process can be derived from the product of the two individual interaction probabilities. A knockout cross section of about 50 mb was derived from our experiment, while a neutron pickup cross section of about 2.5 mb was measured at similar beam energy for the *sd*-shell nucleus ^{22}Mg [32]. It follows that the TS mechanism would have a rather low cross section, of the order of 0.10 mb, that is a factor of 20 lower than we observe for the sum over all states with shifted momentum distributions. It is therefore likely that a more direct process is needed to account for the measured cross section.

Charge-exchange reactions occur more favorably with an allowed GT operator (ΔL=0, ΔJ=0,$\pm$1, $\Delta\pi$=no) that would lead to the production of 1^+ states in ^{36}P starting from the 0^+ ground state of ^{36}S. Higher momentum transfers are also observed when very strict kine-

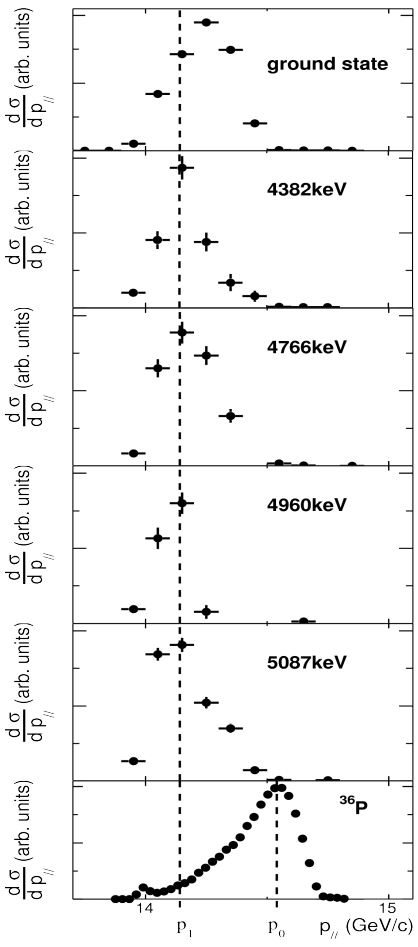

FIG. 4: Measured parallel momentum distributions for the ground state and the states at 4382, 4766, 4960 and 5096 keV (displayed in red in the level scheme) of ^{35}P. The bottom panel shows that for ^{36}P nucleus, as produced from ^{36}S. The vertical dashed line, crossing all panels, represents the centroid of the momentum distribution of ^{36}P nucleus, p_0, shifted by the evaporation of a neutron, i.e. p_1=(A-1)/A p_0. It is seen that the distributions for all states labeled red in the level scheme are shifted relative to that of the ^{35}P ground state, that is produced via direct one-proton knockout.

matic condition for the reaction as well as suitable target excitations cannot be selected, as in the present experiment. Moreover, having a closed neutron *sd* shell, the exchange of an *sd* proton to an *sd* neutron orbital that would lead to 1^+ states in ^{36}S is strongly hindered by Pauli blocking. Rather, transfer to the *fp* or to the highest $g-sd$ orbits must become largely competitive. The non-feeding of any of the known 1^+ states in ^{36}P but the population of the negative parity states 4^- (g.s.), 3^- (250 keV) and of the tentatively assigned 2^- (425 keV) through low-energy charge-exchange reactions of Ref. [33] are in line with the above assumptions. In the present experiment, several γ rays are observed in coincidence with ^{36}P (see Fig. 5). However, none of them

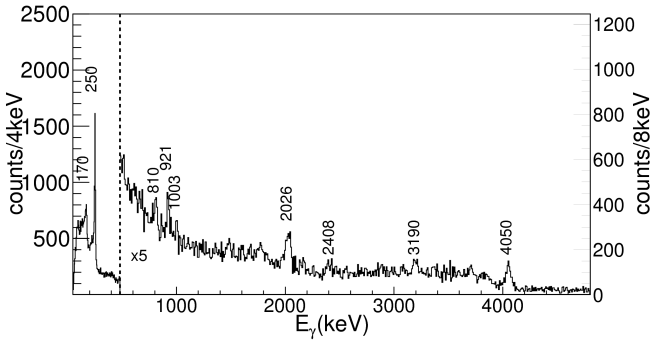

FIG. 5: Doppler-corrected γ-decay spectrum for the ^{36}P nucleus populated from ^{36}S in a nucleon-exchange reaction.

arise from the deexcitation of the 1^+ states at 1303 keV and 2281 keV that were populated in the β decay of ^{36}Si to ^{36}P [34] and whose decay occurs through γ rays of 878 keV and (934, 977, 1858 keV), respectively, as in Ref. [33]. Even if the present statistics does not allow extracting γ-γ coincidences, the observation of transitions at 250 keV and about 170 keV suggest the feeding of the 3^- and 2^- states, respectively. Other transitions are observed, but none (except perhaps the 2020(20) keV from [35]) were reported in previous works. Interestingly, one transition is seen at 4050 keV, i.e. about 600 keV above the neutron emission threshold of 3.465 MeV. This state seems to decay preferentially through a γ-ray transition rather than neutron decay to the $1/2^+$ ground state of ^{35}P.

The last hypothesis is that these momentum-shifted distributions result from the proton knockout from a state excited in inelastic scattering. Such a TS reaction was discussed as one possibility to account for the observation of a γ-decaying neutron-unbound state in ^{35}Si at 3.611 MeV (S_n=2.470(40) MeV) populated in the ^{36}Si $(-1n)$ reaction [22]. As shown in Fig. 4 of Ref. [22], the momentum distribution associated with the production of this unbound state appears to lie dominantly in the low-momentum tail of the ^{35}Si distribution, possibly indicating that its centroid is shifted to lower momentum. The production of such a state was evaluated in Ref. [22] to be of 0.8(2) mb, a value that is comparable to the partial cross sections for the states which are observed with a shifted momentum distribution in our work. A total cross section of 2.4(4) mb is indeed obtained by summing over the four states represented in red in Fig. 2. Contrary to the case presented in Ref. [22], the states here possibly produced by the same TS mechanism are below the neutron separation energy. This could be due to the fact that the neutron emission threshold of ^{35}P (S_n=8.380 MeV) is much higher than the one of ^{35}Si (S_n=2.470 MeV).

VI. CONCLUSIONS

The spectroscopy of ^{35}P was investigated with an intermediate-energy one-proton knockout reaction using a secondary beam of ^{36}S interacting with a ^{9}Be foil at 88 MeV/u mid-target energy. The ^{35}P nuclei were selected by the S800 spectrograph at NSCL and identified in the spectrograph's focal plane in coincidence with prompt γ rays detected in the GRETINA segmented Ge array around the target. The level scheme of ^{35}P has been established up to about 7.5 MeV from γ-γ coincidences and relative γ intensities. Spins and parities for most of the populated states were proposed from a comparison between calculated and measured γ-gated momentum distributions for the population of individual final states in ^{35}P. Spectroscopic factor values, C^2S, were derived from partial cross sections for the $1/2^+$ ground state and the excited states ($3/2^+$, $5/2^+$ and tentatively $1/2^-$) in ^{35}P. An inclusive cross section of 51(1) mb was measured for ^{35}P produced from ^{36}S. The extracted summed $\sum C^2S$ values agree with expected shell-model occupancies of the protons in the $2s_{1/2}$ ($\sum C^2S$=2.2(7)), $1d_{3/2}$ (0.7(3)), $1d_{5/2}$ (5.2(9)) orbitals, while only a fraction (0.41(17)) of the strength corresponding to the deeply-bound $1p_{1/2}$ orbit is tentatively observed for two states above 5.6 MeV.

The present results were compared to those obtained for ^{35}P using the ^{36}S(d,^{3}He)^{35}P transfer reaction at low energy. Remarkable agreement is found for the proposed level scheme populated, the spin assignments (except for one state) and the deduced C^2S values. Since obtained from high-resolution γ-ray spectroscopy, the excitation energies of the presently identified states in ^{35}P are more accurate than those obtained in the (d,^{3}He) reaction [16]. They agree with the values obtained in a multi-nucleon transfer reaction [25], for which several states were observed in common. The present sensitivity of the knockout reaction, with a projectile beam of 2 $\cdot 10^5$ pps, matches the one obtained in the (d,^{3}He) reaction with a d beam on a stable ^{36}S target. This reinforces the enormous potential of this experimental technique in extracting level schemes, orbital angular momenta, and C^2S values.

Besides the observation of states that were expected to be produced in the knockout of protons from the $p-sd$ shell, other states with likely high spin value ($J \geqslant 5/2$) and negative parity are observed as well, with a summed partial cross section of about 2.4 mb. Owing to the facts that these states were not observed in the (d,^{3}He) reaction and that they exhibit parallel-momentum distributions that are down-shifted as compared to the ones from knockout, we propose that they are produced by another mechanism that could be either a charge-exchange or a two-steps mechanism in which a core excitation is followed by a proton knockout. While so far we cannot clearly identify which of these two mechanisms is the most probable, it interestingly leads to the production of states most likely corresponding to neutron-core excitations. This feature may be very interesting to single-out intruder states belonging to the so-called island of inversion, as evoked in Refs. [22, 37].

Acknowledgments

This work is supported by the National Science Foundation (NSF) under Grant Nos. PHY-1102511 and PHY-1306297 and by the Institut Universitaire de France. GRETINA was funded by the US DOE - Office of Science. Operation of the array at NSCL is supported by NSF under Cooperative Agreement PHY-1102511 (NSCL) and DOE under grant DE-AC02-05CH11231 (LBNL). O.S wish to thank T. Duguet for fruitful discussions. J.A.T acknowledges support of the Science and Technology Facility Council (UK) grant ST/L005743.

[1] Y. Uozumi *et al.*, Phys. Rev. C **50**, 263 (1994).
[2] Y. Uozumi *et al.*, Nucl. Phys. A **576**, 123 (1994).
[3] V.R. Pandharipande et al., Rev. Mod. Phys. **69**, 981 (1997).
[4] C. Barbieri, Phys. Rev. Lett. **103**, 202502 (2009).
[5] W. H. Dickhoff and C. Barbieri, Prog. Part. Nucl. Phys. **52**, 377 (2004).
[6] Th. Duguet, H. Hergert, J. D. Holt and V. Somá, Phys. Rev. C **92**, 034313 (2015).
[7] L. Lapikás, Nucl. Phys. A**553**, 297 (1993).
[8] B. P. Kay, J. P. Schiffer and S. J. Freeman, Phys. Rev. Lett. **111**, 042502 (2013).
[9] P.G. Hansen, J.A. Tostevin, Annu. Rev. of Nucl. and Part. Sci. **53**, 219 (2003).
[10] J. A. Tostevin, J. Phys. G: Nucl. Part. Phys. **25**, 735 (1999).
[11] G. J. Kramer, H. P. Blok, and L. Lapikás, Nucl. Phys. A**679**, 267 (2001).
[12] J. A. Tostevin and A. Gade, Phys. Rev. C **90**, 057602 (2014).
[13] J. Lee *et al.*, Phys. Rev. Lett. **104**, 112701 (2010).
[14] F. Flavigny *et al.*, Phys. Rev. Lett. **110**, 122503 (2013).
[15] F. M. Nunes, A. Deltuva, and June Hong, Phys. Rev. C **83**, 034610 (2011).
[16] S. Khan *et al.*, Phys. Lett. B **156**, 155 (1985).
[17] A. Stolz *et al.* Nucl. Instr. and Meth. B **241**, 858 (2005).
[18] D. J. Morrissey, Nucl. Instr. and Meth. B **204**, 90 (2003).
[19] J. Yurkon *et al.*, Nucl. Instr. and Meth. A, **422**, 291 (1999).
[20] M. Berz *et al.*, Phys. Rev. C **47**, 537 (1993).
[21] S. Paschalis *et al.*, Nucl. Instr. and Meth. A **709**, 44 (2013).
[22] S. R. Stroberg *et al.,*, Phys. Rev. C **90**, 034301 (2014).
[23] S. Agostinelli *et al.*, Nucl. Instr. and Meth. A **506**, 250 (2003).
[24] J. P. Dufour *et al.*, Z. Phys. A **324**, 415 (1985).
[25] M. Wiedeking *et al.*, Phys. Rev. C **78**, 037302 (2008).
[26] A. Gade *et al.*, Phys. Rev. C **77**, 044306 (2008).
[27] J. A. Tostevin, Nucl. Phys. A **682**, 320c (2001).
[28] B. A. Brown, Phys. Rev. C **58**, 220 (1998).
[29] C. A. Bertulani and P. G. Hansen, Phys. Rev. C **70**, 034609 (2004).
[30] C. A. Bertulani and A. Gade, Comput. Phys. Commun. **175**, 372 (2006).
[31] A. Gade *et al.*, Phys. Rev. Lett. **102**, 182502 (2009).
[32] A. Gade *et al.*, Phys. Rev. C **83**, 054324 (2011).
[33] L. K. Fifield *et al.*, Nucl. Phys. A **552**, 125 (1993).
[34] J. P. Dufour *et al.*, Z. Phys. A **324**, 487 (1986).
[35] N. A. Orr *et al.*, Nucl. Phys. A **477**, 523 (1988).
[36] E. K. Warburton and J. A. Becker, Phys. Rev. C **35**, 1851 (1987).
[37] R. G. T. Zegers *et al.*, Phys. Rev. Lett. **104**, 212504 (2010).